

Article

Assessing the Impact of Rutting Depth of Bituminous Airport Runway Pavements on Aircraft Landing Braking Distance during Intense Precipitation

Emanuele Toraldo *, Misagh Ketabdari , Gianluca Battista and Maurizio Crispino 

Department of Civil and Environmental Engineering, Politecnico di Milano, Piazza Leonardo da Vinci 32, 20133 Milan, Italy

* Correspondence: emanuele.toraldo@polimi.it

Abstract: A runway pavement during its useful life is subject to a series of deteriorations because of repeated load cycles and environmental conditions. One of the most common deteriorations is the formation of rutting (surface depression in the wheel path) on the runway surface. Rutting negatively affects aircraft performance during landings and will behave even worse during precipitation or with the existence of fluid contaminations on the surface. This paper aims to develop a model for calculating aircraft braking distance during landing on wet-pavement runways affected by rutting based on dynamic skid resistances generated by tire–fluid–pavement interactions. Intense precipitation, variable rutting depths for a 100 m length step, water film depths (e.g., 1 to 26 mm), and aircraft wheel loads (e.g., 10 to 140 kN) are considered as the boundary conditions of the developed model. The output is a model that can estimate aircraft braking distance as a function of rutting depth and can perform further assessment of the probability of the occurrence of landing overrun. After validating the model with existing methodologies and calibrating it according to the actual landing distance required for each type of aircraft, an Italian airport is simulated using a model with real data regarding the level of service of its pavement surface characteristics.



Citation: Toraldo, E.; Ketabdari, M.; Battista, G.; Crispino, M. Assessing the Impact of Rutting Depth of Bituminous Airport Runway Pavements on Aircraft Landing Braking Distance during Intense Precipitation. *Designs* **2023**, *7*, 41. <https://doi.org/10.3390/designs7020041>

Academic Editors: Emadaldin Mohammadi Golafshani and Pedro Aires Montenegro

Received: 10 November 2022

Revised: 20 December 2022

Accepted: 2 March 2023

Published: 6 March 2023



Copyright: © 2023 by the authors. Licensee MDPI, Basel, Switzerland. This article is an open access article distributed under the terms and conditions of the Creative Commons Attribution (CC BY) license (<https://creativecommons.org/licenses/by/4.0/>).

Keywords: aircraft landing braking distance; tire–fluid–pavement interaction; rutting depths; dynamic skid resistance; runway friction; wet runway pavement

1. Introduction and Literature Review

The principal goal of busy airport infrastructures (e.g., runways), as complex transportation systems, is to satisfy the daily demands of freight/passenger transportation by ensuring the safety of operations and passengers' comfort. In other words, guaranteeing the safety of operations should have the highest priority for any airport authority. Therefore, a risk assessment must be integrated into all airport construction and operation phases, which requires transversal skills in several areas due to the large number of involved parameters.

Among all phases of flight (e.g., takeoff, cruise, approach, etc.), landing an aircraft is one of the most critical maneuvers in the aeronautical field due to the high touchdown speeds and heavy aircraft weights involved. According to registered incidents/accidents databases, the most frequent runway-related accident is landing overrun [1], which is directly related to the difference in landing distance available on the runway and the actual landing braking distance of each specific aircraft. In this regard, runway surface characteristics and its level of service play significant roles in aircraft braking potential.

The sufficient braking potential of aircraft can be guaranteed through the activation of aerodynamic brakes, reverse thrust of engines, mechanical brakes, and tire–pavement interaction (i.e., friction force). The surface conditions of the runway pavement, therefore, have a noticeable impact on aircraft landing braking distance.

A runway pavement during its useful life is subject to a series of deteriorations because of repeated load cycles and environmental conditions, and one of the most common deteriorations of bituminous pavements is the formation of rutting on the runway surface. Rutting appears as surface pavement depression in the wheel path, mainly due to the combined effects of airplane loads and high environmental temperatures during summer. Rutting evolution can be divided into two main steps: post-compaction of the wearing course and squeezing of the hot-mix asphalt on the surface of the wearing course. Rutting negatively affects aircraft performance, and it will perform even worse during precipitation or with the existence of fluid contaminations on the runway surface. Of course, other types of pavement distresses (such as crocodile cracking or potholes) can affect pavement drainage capacity; however, it is supposed that in an airport environment, such distresses are not common due to the high attention paid by airport authorities to runway surface characteristics for safety matters. Other examples of pavement distresses mentioned above are mainly common for road pavements; thus, they are not included in the research herein described.

The drainage capacity of a runway, which determines the accumulated water thickness on the surface, is dependent firstly on the precipitation intensity, runway transversal slope, and mean texture depth of the pavement and the rutting depth.

The main scopes of this research can be divided into, first, analyzing the interactions between the aircraft main gear wheel and the runway pavement in the case of heavy rain, since the existence of any contamination on the runway surface would compromise aircraft performance during landing, and second, evaluating the negative impacts of pavement distresses (i.e., rutting) on runway friction.

For this matter, an accurate analysis of the literature is performed to study the proposed methodologies by other researchers. Throughout the literature, many studies have focused on the effects of water contamination on friction, but sufficient attention has not been paid to the impacts of pavement distresses and how they can weaken aircraft braking potential.

In this regard, an analytical model is developed to simulate tire–fluid–pavement interactions to estimate the braking distance of aircraft during landing on wet-pavement runways affected by rutting. Intense precipitation, variable rutting depths for a 100 m length step, water film depths (e.g., 1 to 26 mm), and aircraft wheel loads (e.g., 10 to 140 kN) are considered as the boundary conditions of the developed model. The output is a model that can estimate aircraft braking distance as a function of rutting depth and can perform further assessment of the probability of the occurrence of landing overrun. After validating the model with existing methodologies and calibrating it according to the actual landing distance required for each type of aircraft, an Italian airport is simulated using a model with real data regarding the level of service of its pavement surface characteristics.

According to the available scientific literature, several studies have been carried out over the past years with the aim of evaluating the probability of the occurrence of runway-related accidents in different boundary conditions (aviation risk assessment).

In 2011, Valdés et al. [2] developed an accident risk model using a probabilistic approach. The authors collected recorded incident data from different sources into a database and then correlated the data with traffic data. The analysis period chosen is 23 years from 1984 to 2007. Table 1, which is extrapolated from this study, shows the percentages of accidents assigned to the different phases of flight.

Table 1. Accident shares of each phase of flight [2].

Phase of Flight	Accident Percentage
Taxiing	4%
Takeoff	14%
Climb	13%
Cruise	10%
Descent	2%
Approach	27%
Landing	30%

According to this table, the most critical phase of flight is landing.

In 2003 and 2004, Kirkland et al. [3,4] gave an important contribution to airport risk analysis by developing a model that is based on a normalized and corrected database of accidents and various boundary conditions (e.g., pavement type, runway geometry, aircraft characteristics, etc.). The model, which mainly evaluates runway excursion accidents due to unsuccessful takeoffs and landings, has three components, comprising probability of occurrence, wreckage location, and severity of consequences. The results of the study confirm the applicability of the model to analyze the risk of runway excursions for limited boundary conditions. Therefore, it is not possible to introduce all desired boundary conditions (e.g., pavement level of service, weather, etc.) to the model.

In 2007 and 2008, Ong and Fwa [5,6] studied the influence that the presence of a film of water on the pavement can have on traffic safety, considering both motorways and runways. By investigating the phenomenon of hydroplaning and the reduction of the slip coefficient caused by the presence of water on the pavement, the authors developed a model to evaluate the pneumatic–water–pavement interaction, and it was validated using two reference empirical formulas for the calculation of hydroplaning proposed by Horne and Dreher in 1963 [7] and Horne et al. in 1986 [8]. Although the developed model offers many improvements with respect to the previous studies, it is functional with limited choices of water film thicknesses (WFTs) and aircraft wheel loads.

The presence of a water film on the runway pavement has significant consequences, even if the hydroplaning phenomenon does not occur, such as a decrease in skid resistance, which leads to an increase in aircraft braking distances. In 2011, Pasindu et al. [9] analyzed aircraft braking distances in the presence of various water films on the runway surface by proposing a finite-element model that calculates dynamic skid numbers with the variation of aircraft speed. This model, which simulates the 3D footprint of the aircraft main gear wheel on a wet surface, is based on the pneumatic–water–pavement interaction model proposed by Ong and Fwa [6]. As before, the developed model is still applicable to a limited choice of WFTs and wheel loads.

In 2018, Ketabdari et al. [10] collected a comprehensive database of airport ground maneuver accidents/incidents. After that, precise sensitivity analyses based on this database were performed by the authors to discover the most influential parameters on the risk of aircraft operations. As a result of this study, meteorological conditions and runway geometry were selected as the two most impactful variables on the surface conditions of a pavement, respectively, with a consequent increase in the probability of the occurrence of excursion accidents, especially at high aircraft speeds. In 2019, the authors created a risk model based on the outputs of previously performed sensitivity analyses [11] and the aircraft braking distance model proposed by Pasindu et al. [9]. This risk model improved the previous restrictions related to the applicable ranges of WFTs and wheel loads, and it estimates aircraft braking distance during landing on a wet runway, but only for a flat runway surface.

In 2021, Ketabdari et al. [12] analyzed the influences of the longitudinal and transverse slopes of a runway on drainage capacity under intense precipitation conditions and improved the previously proposed braking distance model. The results obtained show how the longitudinal slope has an insignificant effect on the water veil flow path on the

pavement, while the runway transverse slope is a fundamental parameter for calculating the thickness of the water veil.

Due to the heavy loading cycles present on a runway, the formation of ruts is one of the main deteriorations that a runway is subject to. Ruts are caused by the accumulation of permanent deformations in the pavement layers that occur along the paths of the wheel passages through the formation of grooves on the surface. In 2016, Pasindu et al. [13] analyzed the influence of rutting depths (5, 10, 15, and 20 mm) on the hydroplaning risk in the ground operations of aircraft (100, 125, and 150 kN wheel loads). The results demonstrate that the risk of hydroplaning due to the presence of ruts is present only in the early stages of the landing maneuver, where speeds are much higher.

The presence of ruts on a pavement and how it modifies the disposal of surface water has been studied over the years mainly in the road sector. In 2020, Alber et al. [14] created a three-step model for assessing the drainage capability of a pavement that has ruts. In the first phase, the behavior of the pavement material is characterized, which then, in the second phase, is inserted into a finite-element model (pneumatic–pavement interaction) to evaluate its long-term behavior, predicting the inelastic deformations accumulated on the pavement surface. In the final phase, the deformations obtained in the previous step are used to calculate the thickness of the water film present on the pavement.

Keeping in mind that the ruts on a pavement always occur in pairs (on the passage paths of the wheels), it should be considered that the two ruts may not always be in the same conditions. In 2022, Zhang et al. [15] investigated the risk associated with a situation in which one track is full of water and the other remains dry, considering the lateral stability of the vehicle resulting from this situation. In the study, a dynamic model of the vehicle was developed, which considers the difference between the coefficients of friction between the two tracks. The study shows that the width and length of a rut trail are the most significant influential parameters on the risk associated with rutting.

2. Model of the Aircraft Landing Braking Distance

The model proposed in this study, which calculates aircraft braking distance over a runway affected by the rutting phenomenon in intense precipitation, consists of four sub-models:

1. Calculative model of WFTs in various precipitations;
2. Calculative model of accumulated water thickness in ruts;
3. Interpolative model of dynamic skid resistance in different WFTs and speeds;
4. Simulative model of aircraft braking distance in wet/deteriorated pavement.

The braking potential of civil aircraft plays a significant role in total landing distance. It is highly dependent on the surface conditions of the runway pavement, especially during high-intensity precipitations. The runway surface condition, which depends on real-time weather conditions and pavement level of service, can modify the coefficient of friction between the aircraft wheel and the pavement, increasing or decreasing the distance needed to stop an aircraft [16]. In general, the variables that can influence the braking distance of a landing aircraft can be grouped into three macro categories:

- Aircraft characteristics;
- Pavement characteristics and level of service;
- Weather conditions.

2.1. Calculative Model of WFTs in Various Precipitations

One of the most influential weather conditions on aircraft performance is rainfall. In this regard, the effect of intense precipitation (100 mm/h) considered in the model, compared to a previous study by the authors [12], which was violent precipitation (65 mm/h), leads to upgrading the model to be compatible with worst-case scenarios. As a result of intense precipitation, the thickness of the water film accumulated on the surface depends on not only the intensity and duration of the rainfall, but also the pavement

condition itself. Thanks to the transverse and longitudinal slopes, the flow paths of raindrops are toward the runway lateral borders, as depicted in Figure 1 for a double-pitched even runway.

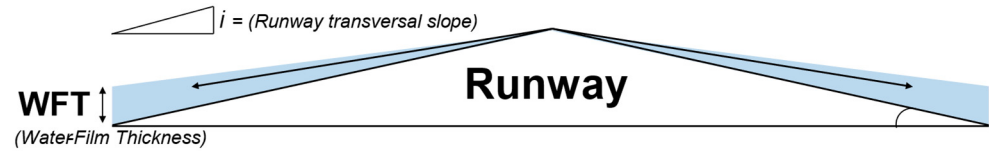


Figure 1. Raindrops outflow from an even runway.

Several empirical and analytical formulas have been developed over the past years for calculating the thickness of the water film on a pavement surface following precipitation of a certain intensity. The formula developed by AASHTO in 1992 [17] is adopted in Sub-Model (1) of this study, as follows:

$$WFT = (0.00338 \times MTD^{0.11} \times L_f^{0.43} \times I^{0.59} \times S_f^{-0.42}) - MTD, \quad (1)$$

where *WFT* represents the thickness of the water film on the pavement (in), *L_f* is the length of the flow path (ft), *I* is the rain intensity (in/h), *S_f* is the slope of the flow path (/), and *MTD* is the mean texture depth (in).

The *MTD*, which can be measured by the volumetric sand patch method, is a measure of surface roughness and known, in good conditions, by values of just over a millimeter. The pavement texture guarantees the friction of vehicles' tires at high sliding speeds and becomes essential, especially in wet surface conditions. As can be seen from Equation (1), deteriorations, such as the rutting phenomenon, to which a pavement may be subjected during its useful life have not been formulated in the equation.

2.2. Calculative Model of Accumulated Water Thickness in Ruts

As mentioned before, the pavement deterioration in question for this study is the rutting phenomenon, which manifests itself on the surface by forming a pair of grooves of varying depths along the tire passage paths due to the repeated transit of aircraft (especially during summer) and can modify the surface runoff of rainwater from the runway itself. A pavement that has ruts will therefore have a lower drainage capacity with respect to a non-deteriorated pavement. During rainfall, water gets stuck in the ruts and causes a consequent decrease in the coefficient of friction.

Flexible pavement, which consists of bituminous layers with different thicknesses, is in fact more vulnerable to rutting with respect to a rigid pavement (i.e., concrete slabs). In general, in an airport, the use of a flexible pavement is preferred for the runways, junctions, and taxiways, while a rigid pavement is mainly adopted for the aprons since the flexible pavement guarantees greater friction while making maintenance interventions easier. In other words, requalifying a flexible pavement mostly can be achieved by just repaving surface layers, while in a rigid pavement, the restoration often requires the complete replacement of the slab.

The runway disposal of rainwater can be strongly interrupted by the presence of ruts on the surface, as illustrated in Figure 2. In the case of intense and long-duration rainfall, water accumulates within the ruts, leading to the formation of a *WFT* higher than that present on the rest of the pavement.

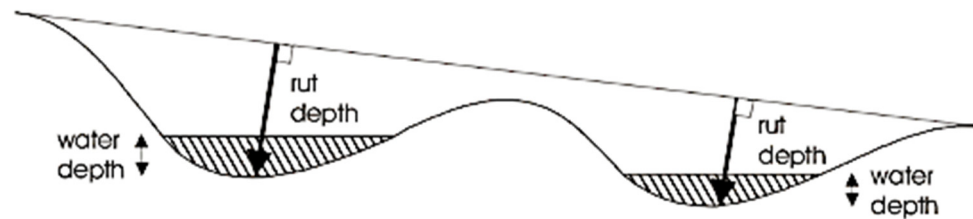


Figure 2. Accumulation of rainfall water in a pair of ruts [18].

As confirmed by several studies [13,14,19,20], during intense rainfall, the pair of ruts will be entirely filled with water as the raindrops move toward runway lateral borders. Therefore, it is reasonable to assume in Sub-Model (2) that over the ruts, the accumulated thickness of water is equal to the depth of the rut, as presented in Equation (2):

$$WFT = RD, \tag{2}$$

where *RD* represents the depth of the rut (mm).

Rutting depth and its location can vary transversely along the runway according to axle load, load cycle numbers, and outer main gear wheel span (OMGWS) of each operating aircraft. Moreover, the depth will not be constant along the longitudinal direction of the runway since, during the takeoff and landing maneuvers, not all sections of the pavement will be loaded in the same way. By generalizing the phenomenon in an airport with uneven traffic, ruts with different depths in the longitudinal direction and at various distances from the runway centerline will be formed. An aircraft normally lands with the nose gear positioned exactly on the runway centerline with the main gear wheels at the same transverse distances from the centerline. Therefore, by comparing the OMGWS of each operating aircraft and the exact location distribution of ruts, it is possible to evaluate whether the wheels pass through the ruts.

The WFT is dependent firstly on the precipitation intensity, runway transversal slope, and the mean texture depth of the pavement and the rutting depth. In other words, the possible volume of water that can accumulate in an existing rut over the runway surface depends on the drainage rate of the runway (based on the transversal slope) after rainfall. The water film thickness that is stock in the rutting is dependent on the RD and the mean texture depth of the pavement, as expressed by the above-mentioned equations. The ruts present on a runway can be measured via a profilometer bar, which is generally mounted on a vehicle that runs along the runway parallel to the runway centerline. The profilometer bar is equipped with a laser that, at a constant pitch, detects the transversal profile of the pavement. By processing the results of the measurement, the depth of the ruts and their distribution for the entire extension of the runway can be obtained. According to ASTM [21], the severity thresholds for this type of deterioration in an airport are presented in Table 2.

Table 2. Severity thresholds of rutting depths [21].

Rutting Depth (mm)	Severity
RD < 13	Low
13 ≤ RD ≤ 25	Medium
RD > 25	High

2.3. Interpolative Model of Dynamic Skid Resistance in Different WFTs and Speeds

After determining how intense rainfall fills the existing ruts over a runway, based on the longitudinal and transverse slopes, and forms different WFTs, the computation of dynamic skid number, affected by considered boundary conditions, should be investigated.

Skid number, which is linked to the pavement friction, depends on the aircraft speed and the WFT, as presented in Equation (3) [9]:

$$SN_v = 100 \times F_x / F_z, \tag{3}$$

where F_x represents the horizontal forces acting on the aircraft (N), and F_z is the vertical forces acting on the aircraft (N).

In the presence of water films over the surface, skid resistance between the tire and pavement has a dynamic nature, and it will be varied according to changes in speed and wheel load (W) of the vehicle. Pasindu et al. [9] proposed the relationship between SN, WFT, and aircraft wheel load, as depicted in Figure 3.

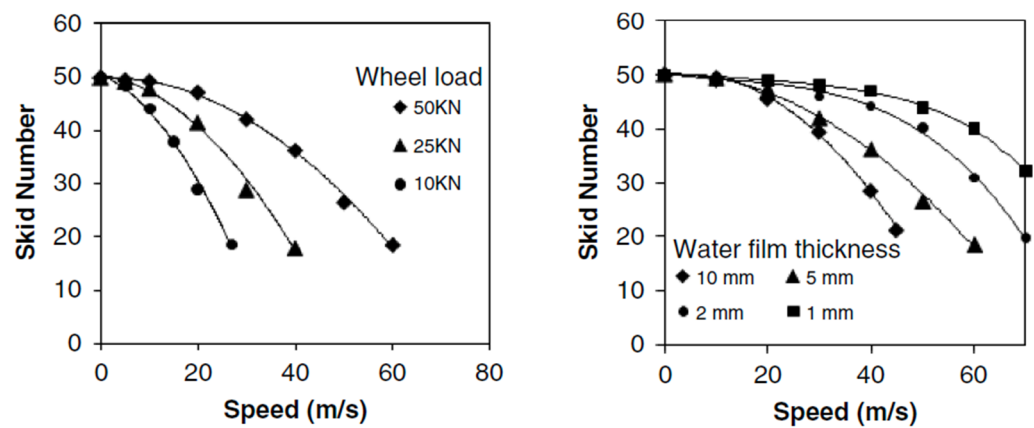


Figure 3. Dynamic skid number versus aircraft speed for various WFTs and wheel loads [9].

As can be interpreted from the figure above, these relationships are applicable only to limited ranges of WFTs and wheel loads. Therefore, to expand these limitations and make the relationships applicable for wider ranges, several interpolation algorithms have been tested in Sub-Model (3) to find the best-fitted one, as presented in Table 3.

Table 3. Tested Fitting relationships for speed versus W and WFT.

Fitting Relationship (Speed: W) (WFT = Const.)	Total Error	Fitting Relationship (Speed: WFT) (W = Const.)	Total Error
$v = aw^b$	17.707%	$v = aWFT^b$	20.038%
$v = aw^b + c$	0.004%	$v = aWFT^b + c$	13.842%
$v = aw + b$	1.452%	$v = aWFT + b$	357.104%
$v = aw^2 + bw + c$	0.000%	$v = aWFT^2 + bWFT + c$	31.508%

By selecting the best-fitted relationship (highlighted ones on the table), in which a, b, and c are the general coefficients, it is now possible to compute the relative skid numbers to speed values for WFTs (from 1 to 26 mm) and aircraft wheel loads (from 10 to 140 kN).

2.4. Simulative Model of Aircraft Braking Distance in Wet/Deteriorated Pavement

After achieving the objectives of the above-mentioned steps, thanks to Sub-Model (4), it is possible to calculate the aircraft braking distance during landing on a wet-pavement runway, which is affected by rutting. This step, which is formulated based on the law of motion, calculates the braking distance through the following principal Equation (4):

$$S = \int_0^T \left[v_b - \left([\mu(v, x)]g + \frac{0.5\rho[v(t)]^2 A(C_D - [\mu(v, x)]C_L)}{MLW} \right) t \right] dt \tag{4}$$

where S represents the aircraft braking distance (m), V_b is the speed of the aircraft at onset of braking (m/s), g is the gravitational acceleration (m/s^2), ρ is the air density (kg/m^3), $v(t)$ is the aircraft speed at time t (m/s), $\mu(v,x)$ is the dynamic coefficient of friction between tire and pavement, A is the wing area (m^2), C_D is the drag coefficient, and C_L is the coefficient of lift.

It is assumed that the aircraft wheel stops rotating as the braking system is activated and the aircraft slides on the pavement due to the water film present on the runway. Therefore, the wheel in this condition has a zero angular speed and a sliding speed equal to that of the aircraft, which can be considered as the worst-case scenario.

Out of the entire duration of landing, only the time span from the moment of touchdown, with horizontal aircraft alignment, till the full stop is adopted in the computations. Moreover, in the model, the interaction of the aircraft main gear with the pavement is considered since the main gear carries approximately 95% of the weight of the aircraft [9,12]. Therefore, Equation (5) is adopted to calculate the weight acting on a single wheel of the aircraft main landing gear (W):

$$W = 0.95 \times (MLW \times g - L)/n, \tag{5}$$

where MLW presents the maximum landing weight (kg), n is the number of wheels in the main gear, and L is the lift (kN), which can be calculated through Equation (6):

$$L = 0.5 \times \rho \times v^2 \times A \times C_L, \tag{6}$$

where v presents the aircraft approach speed (m/s). Therefore, to calculate the aircraft braking distance through Equation (4), MLW should be substituted with W obtained from Equation (5).

In addition, it is assumed that an aircraft lands with the nose gear positioned exactly on the runway centerline. Consequently, the outer main gear wheel span (OMGWS) will be aligned symmetrically with respect to the runway centerline.

The actual simulation of aircraft braking distance is carried out through modeling codes conducted in the MATLAB environment. In other words, several scripts have been conducted, which by collecting the required input variables, return the Gaussian probability distribution of the braking distances of a specific aircraft landing on a pavement for different operation boundary conditions (e.g., different WFTs, MTDs, RDs, and various touchdown speed ranges, as fully described above).

The developed scripts solve Equation (4) for successive time intervals by means of a loop that stops when $V_{(2)}$ is equal to 0, which means the aircraft reaches a full stop. The coefficient of friction $\mu(v,x)$ present in the formula is updated at each time step Δt according to the changes in skid resistance.

The flow chart presented in Figure 4 explains how the developed model works in all its parts, as well as which input data are required for each phase.

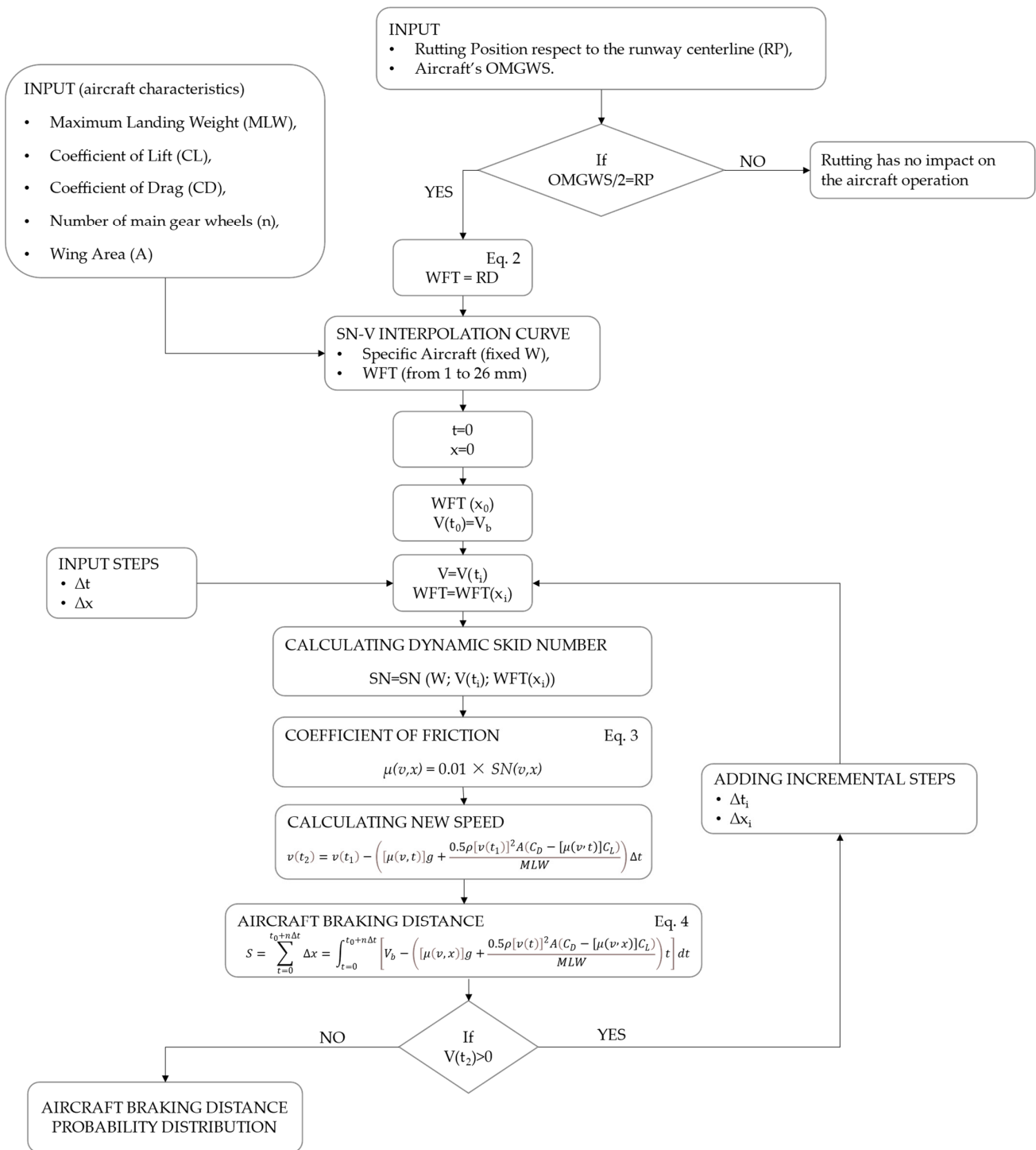


Figure 4. The algorithm of the aircraft braking distance calculation model.

3. Model Validation and Calibration

3.1. Validation Process

To evaluate the precision of the developed model, validating the results is essential. For this matter, the validation process can be carried out by comparing the results obtained with known experimental data, or with similar models present in the literature.

It should be noted that identical models that can evaluate the braking distance of aircraft during landing on a wet and rutted pavement do not exist in the literature, which emphasizes the innovative nature of this study. However, it is possible to find similar

models that compute the braking distance of landing aircraft on wet pavements with limited ranges of WFTs [9,11,12]. Therefore, to validate the precision of the model's results, two different approaches are adopted:

- Comparing the results of wet with dry pavement conditions;
- Comparing the results of the existing model [9] in the literature and the proposed model.

The first validation is made by comparing the probability distributions of the braking distance of an Airbus 320 during landing on a dry pavement ($WFT = 0$ mm) with wet pavement ($WFT = 10$ mm). In the dry surface condition, the skid number can be assumed to be constant and equal to SN_0 equal to 50 for any speed [22], while in the presence of a water film thickness of 10 mm on the runway, the dynamic SN values should be calculated from the aforementioned SN-v curve. As a result of this comparison, the mean braking distance is equal to 1051.34 m for the dry condition and 1401.87 m for the wet pavement. According to the results, the proposed model is sensitive to the presence of water by giving back greater braking distances.

The second validation is performed by resimulating the illustrative example presented by Pasindu et al. [9] by the proposed model (aircraft wingspan = 35.80 m; $\rho = 1.224$ Kg/m³; $A = 54$ m²; $MLW = 20.00$ tons; $WFT = 5$ mm; *average touchdown speed* = 55 m/s).

As a result, the mean braking distance calculated by Pasindu et al.'s model is equal to 621 m, while the mean value of 649.9 m is obtained by the proposed model, which shows a difference of less than 30 m (5%).

The combination of the two validations described above made it possible to validate the precision of the developed model.

3.2. Calibration Process

The necessity of applying a calibration factor (C_f) on the primary results of the developed model is inevitable since many simplification assumptions were considered during the development of the model. Therefore, this calibration factor will normalize the results with respect to the real aircraft braking distance. To calculate the calibration factor, the landing distance required (LDR) for each type of operating aircraft at an airport under study should be extracted from the aircraft performance planning report of the Airbus 320, where 1650 m is required as a safe landing distance of such aircraft. The LDR must guarantee the safety of operations in any condition (by a safety factor of 1.43 [23]). C_f should be computed for each type of aircraft separately by Equation (7):

$$C_f = LDR_{adj}/S_{mean}, \quad (7)$$

where S_{mean} presents the calculated mean braking distance for an aircraft with $C_f = 1$.

As an example, the calculated braking distance (S_{mean}) for Airbus A300–600 by the proposed model is 874.54 m, while according to the aircraft performance planning report of the same aircraft, the LDR is 1532.00 m. By applying the above-mentioned safety factor of 1.43 on the LDR, the adjusted LDR will be 1071.33 m. Finally, the C_f adopted for A300–600 will be $1071.33/874.54 = 1.225$.

4. Case Study Simulation

In this section, an international Italian airport is selected as the case study to be simulated through the developed model. Therefore, the braking distances of the operating aircraft at this airport during landing on its wet and rutted runway are calculated. In this regard, intense rainfall (100 mm/h) is considered as the weather condition of the simulation. This simulation is needed to evaluate the functionality of the developed methodology, as well as to explain in even more detail the procedure to be followed for using the model.

Initially, the input data are collected from the case study; then, these data are analyzed and inserted into the model to simulate the landing braking distance of each type of aircraft. Finally, the results obtained from the model are demonstrated in the form of probability distributions of the braking distances for different aircraft.

4.1. Input Data

The depths of the ruts (RD) present on the runway surface are measured through a multi-functional vehicle (MFV), which evaluates the pavement condition by moving over it at a speed of approximately 50 km/h. The MFV is equipped with 17 lasers installed on a profilometric bar by means of which the transverse regularity of the surface can be measured with a constant sampling step. The bar allows investigating a width of 4 m. In the adopted survey scheme, each passage of the vehicle investigates 3.75 m while maintaining 0.25 m of overlap to avoid the loss of information. RDs were measured on two main alignments, respectively, 3 m and 6 m, to the right and to the left of the runway centerline. The obtained data are therefore represented by the depth of the ruts over these two alignments and with a longitudinal sampling step equal to 10 m, as partially presented in Table 4. It should be noted that the ruts measured on the runway of the selected airport have a maximum depth of 9 mm, indicating a pavement in good condition and with a low-risk severity, according to Table 2, which confirms the safety of operations.

Table 4. An exemplary extraction of rutting depths values registered for the case study.

RD Value (mm)		Alignment from Centerline			
		LEFT		RIGHT	
From (km)	To (km)	6.00 (m)	3.00 (m)	3.00 (m)	6.00 (m)
0.00	0.01	5.00	4.00	5.00	3.00
0.01	0.02	4.00	4.00	6.00	3.00
0.02	0.03	6.00	5.00	7.00	4.00
0.03	0.04	3.00	3.00	7.00	3.00
0.04	0.05	4.00	3.00	8.00	3.00
0.05	0.06	4.00	3.00	6.00	3.00
0.06	0.07	4.00	1.00	6.00	2.00
0.07	0.08	4.00	1.00	5.00	2.00
0.08	0.09	3.00	2.00	5.00	1.00
0.09	0.1	2.00	2.00	7.00	2.00

Among all aircraft operating at the airport, the five most frequent ones are selected to be analyzed since they are responsible for approximately 95% of total movements. The characteristics of these aircraft are presented in Table 5.

Table 5. The main characteristics of the most frequent operating aircraft at selected airport.

Aircraft	ICAO Class	Wingspan (m)	Length (m)	Wing Area (m ²)	N° Wheels	OMGWS (m)	MLW (ton)	Frequency (%)
Airbus 300–600	D	44.84	54.08	260.00	8	10.97	138.00	2.19
Airbus 320	C	35.80	37.57	122.00	4	8.95	67.40	8.26
Airbus 321	C	35.80	44.51	122.60	4	8.97	79.20	1.88
Boeing 737–800	C	34.80	39.50	124.60	4	7.00	63.32	80.09
Boeing 757–300	D	38.05	54.47	185.30	8	8.53	101.61	2.15

4.2. Application

Initially, the distance between the OMGWS of each aircraft should be compared with the registered alignments of the ruts present on the runway. In this regard, the values of rutting depth registered at 6 m from the runway centerline are considered for Airbus 300–600, while those values related to 3 m from the runway centerline are considered for the rest of the aircraft.

The weight and lift forces acting on a single wheel of the landing main gear of each aircraft are calculated by means of Equations (5) and (6), respectively, as presented in Table 6.

Table 6. Weight and lift forces acting on a single wheel of the main gear.

Aircraft	W (kN)	L (kN)
Airbus 300–600	123.69	321.14
Airbus 320	124.05	138.86
Airbus 321	149.06	149.33
Boeing 737–800	107.79	167.30
Boeing 757–300	90.41	235.45

The SN-v curves are acquired for each type of aircraft by adopting the interpolation processes explained in Section 3. For instance, the SN-v curve of Airbus 300–600 is presented in Figure 5.

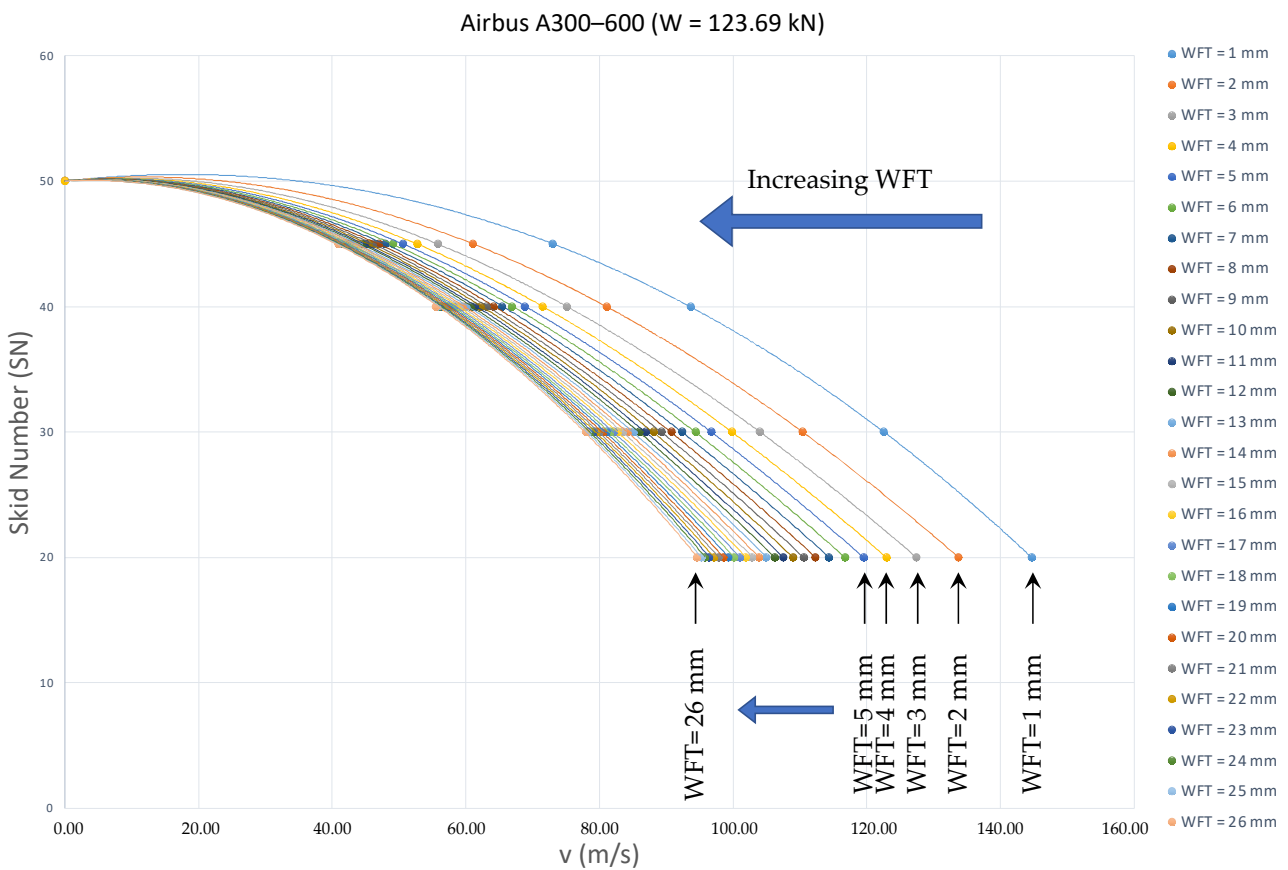


Figure 5. SN-v curve of Airbus A300–600 for different WFTs.

After providing all the required input data to execute the MATLAB script, the braking distance corresponding to the selected five aircraft on the runway of the case study is computed. The spatial and temporal discretization adopted in the calculation, which are equal for all the cases considered, are as follows:

- $\Delta t = 0.3$ min;
- $\Delta x = 100$ m.

After obtaining the braking distances of each selected aircraft under certain adopted boundary conditions, these primary values should be calibrated through Equation (7).

Therefore, different calibration factors are assessed for each aircraft, according to their LDR values, and reduced by a safety factor equal to 1.43, as presented in Table 7.

Table 7. Assessed calibration factors for each aircraft.

Aircraft	$S_{C_f=1}$ (m)	LDR (m)	C_f
Airbus 300–600	874.54	1532	1.2250
Airbus 320	793.65	1650	1.4538
Airbus 321	1083.19	1850	1.1943
Boeing 737–800	684.18	1600	1.6354
Boeing 757–300	845.40	1800	1.4889

The values of the braking distances (S) represent the average values of the probability distributions of the braking distances that are obtained for each aircraft using a calibration coefficient of 1 and a water film thickness of 1 mm.

5. Results and Discussion

The average values of the braking distance of the aircraft reported in Table 7 under the selected boundary conditions are as follows.

- Airbus 300–600, $S_{(average)} = 1175.69$ m;
- Airbus 320, $S_{(average)} = 1266.91$ m;
- Airbus 321, $S_{(average)} = 1409.20$ m;
- Boeing 737–800, $S_{(average)} = 1255.54$ m;
- Boeing 757–300, $S_{(average)} = 1526.78$ m.

Moreover, all probability distributions of the braking distances of those five selected aircraft are calculated, and the results for Airbus 300–600 and Boeing 757–300 are provided in Figures 6 and 7 as examples.

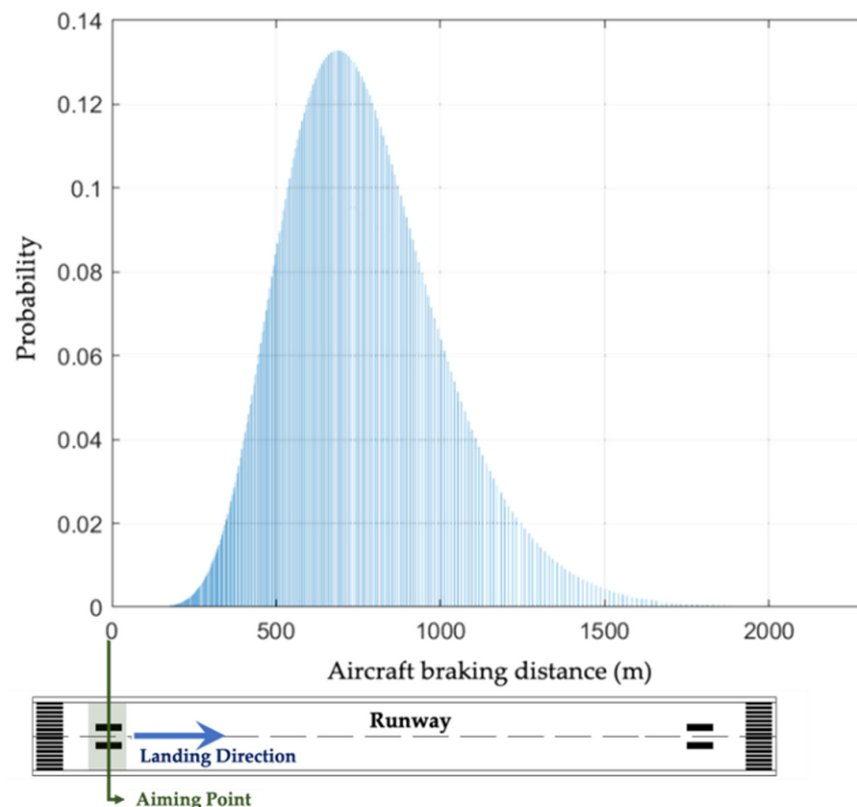


Figure 6. Probability distribution of the braking distances of Airbus 300–600, projected on a 2000 m runway.

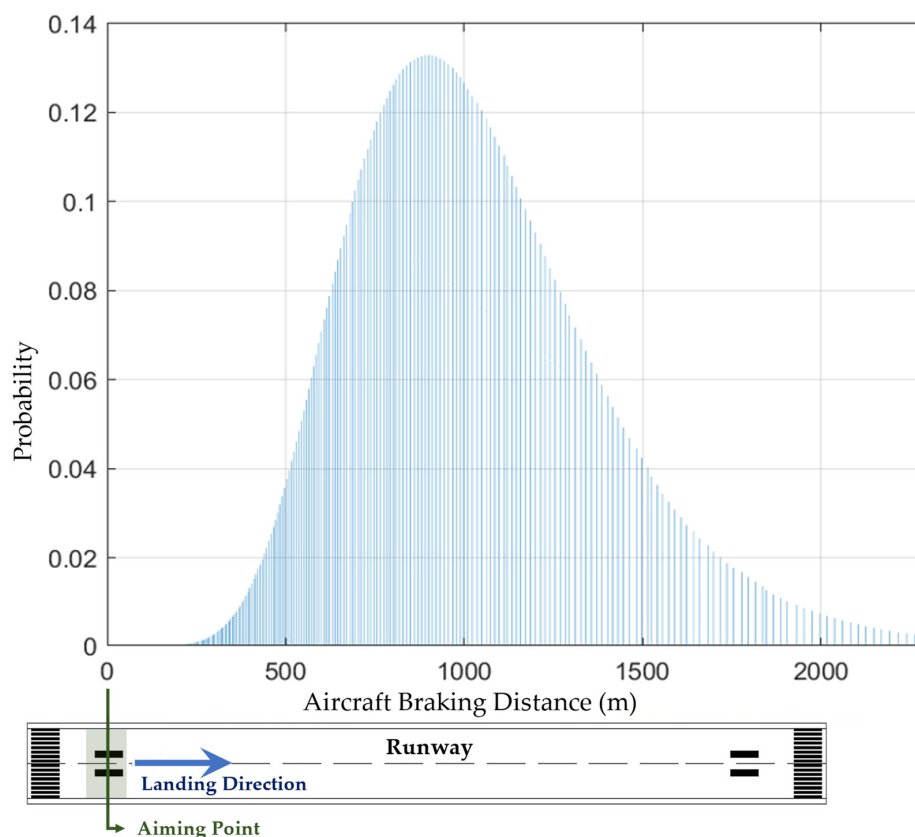


Figure 7. Probability distribution of the braking distances of Boeing 757-300, projected on a 2000 m runway.

According to the results, Boeing 757-300 on average experiences longer braking distances with respect to Airbus 300. It should be noted that each aircraft moves over a different rutting alignment with respect to the other aircraft. In other words, the outer main gear of Airbus 300-600 passes over the rutting presented at 6 m from the runway centerline and Boeing 757 at 3 m from the runway centerline. In fact, existing ruts at 3 m away from the runway centerline are deeper with respect to those at 6 m, which leads to the presence of thicker water films under wheels with a consequent increase in the braking distances.

Moreover, the weight of the aircraft tends to decrease the water film thickness present under the wheels; thus, the value of the dynamic skid coefficient increases. In fact, the increase in SN leads to a decrease in aircraft braking distance. Airbus 300-600 and Boeing 757-300 have wheel loads of 123.69 kN and 90.41 kN, respectively. The results show that a smaller wheel lead causes longer braking distance.

In these calculations, the rutting depths are collected for each 100 m of the entire runway length, according to the extracted real data from the case study, as demonstrated partially in Table 4.

6. Conclusions

In this study, an analytical model for calculating the braking distance of landing aircraft on a wet and rutted runway is proposed. The model considers the depth of ruts present on the pavement surface through the hypothesis of adopting a water film thickness equal to the rutting depth.

Intense precipitation, variable rutting depths for a 100 m length step, water film depths (e.g., 1 to 26 mm), and aircraft wheel loads (e.g., 10 to 140 kN) are considered as the boundary conditions of the developed model.

The outputs are the probability distributions of braking distance, useful for performing a quantitative risk assessment of the ground operation of aircraft. In fact, by comparing the length of a given runway, with the braking distances obtained from the model, it is possible

to calculate the probability of runway excursions (i.e., overruns) by a given aircraft. Furthermore, by defining the exact position of obstacles present in the runway surroundings, the probability that a certain aircraft will hit a specific obstacle can be obtained. Moreover, the development of this model aims to identify the acceptable threshold of the rutting depths for aircraft maneuvers in intense precipitation conditions on a particular runway by evaluating the possible consequences (e.g., an increase in aircraft braking distance during landing).

It should be noted that identical models that can evaluate the braking distance of aircraft during landing on a wet and rutted pavement do not exist in the literature, which emphasizes the innovative nature of this study. However, it is possible to find similar models that compute the braking distance of landing aircraft on wet pavements but with limited ranges of WFTs. Therefore, compared to the existing models, the proposed model is not only capable of considering a noticeably wider range of WFTs, but it can also apply the effect of rutting depth in the braking distance calculation.

Thanks to this model, it is also possible to evaluate the efficiency of runway junction locations by superimposing the obtained Gaussian probability distribution of aircraft braking distance on the runway plan to assess the most optimum area to exit from the runway. An analysis of this type can be useful both in the preliminary design phase of new airport infrastructures (i.e., runways) or in maintenance interventions of an existing airport.

Author Contributions: Conceptualization, E.T. and M.K.; methodology, E.T. and M.K.; software, M.K. and G.B.; validation, E.T., M.K. and G.B.; formal analysis, M.K. and G.B.; investigation, M.K. and G.B.; resources, M.K. and G.B.; data curation, M.K. and G.B.; writing—original draft preparation, M.K.; writing—review and editing, E.T.; supervision, E.T. and M.C.; project administration, E.T. and M.C. All authors have read and agreed to the published version of the manuscript.

Funding: This research received no external funding.

Data Availability Statement: Not applicable.

Conflicts of Interest: The authors declare no conflict of interest.

References

1. Ketabdari, M.; Millán, I.P.; Toraldo, E.; Crispino, M.; Perneti, M. Analytical Optimization Model to Locate and Design Runway-Taxiway Junctions. *Open Civ. Eng. J.* **2021**, *15*, 347–359. [\[CrossRef\]](#)
2. Valdés, R.M.A.; Comendador, F.G.; Gordún, L.M.; Nieto, F.J.S. The development of probabilistic models to estimate accident risk (due to runway overrun and landing undershoot) applicable to the design and construction of runway safety areas. *Saf. Sci.* **2011**, *49*, 633–650. [\[CrossRef\]](#)
3. Kirkland, I.; Caves, R.E.; Hirst, M.; Pitfield, D.E. The normalisation of aircraft overrun accident data. *J. Air Transp. Manag.* **2003**, *9*, 333–341. [\[CrossRef\]](#)
4. Kirkland, I.D.L.; Caves, R.E.; Humphreys, I.M.; Pitfield, D.E. An improved methodology for assessing risk in aircraft operations at airports, applied to runway overruns. *Saf. Sci.* **2004**, *42*, 891–905. [\[CrossRef\]](#)
5. Ong, G.P.; Fwa, T.F. Wet-pavement hydroplaning risk and skid resistance: Modeling. *J. Transp. Eng.* **2007**, *133*, 590–598. [\[CrossRef\]](#)
6. Fwa, T.F.; Ong, G.P. Wet-pavement hydroplaning risk and skid resistance: Analysis. *J. Transp. Eng.* **2008**, *134*, 182–190. [\[CrossRef\]](#)
7. Horne, W.B.; Dreher, R.C. *Phenomena of Pneumatic Tire Hydroplaning*; National Aeronautics and Space Administration: Washington, DC, USA, 1963; Volume 2056.
8. Horne, W.B.; Ivey, D.L.; Yager, T.J. *Recent Studies to Investigate Effects of Tire Footprint Aspect Ratio on Dynamic Hydroplaning Speed*; ASTM International: West Conshohocken, PA, USA, 1986; pp. 26–46.
9. Pasindu, H.R.; Fwa, T.F.; Ong, G.P. Computation of aircraft braking distances. *Transp. Res. Rec.* **2011**, *2214*, 126–135. [\[CrossRef\]](#)
10. Ketabdari, M.; Giustozzi, F.; Crispino, M. Sensitivity analysis of influencing factors in probabilistic risk assessment for airports. *Saf. Sci.* **2018**, *107*, 173–187. [\[CrossRef\]](#)
11. Ketabdari, M.; Crispino, M.; Giustozzi, F. Probability contour map of landing overrun based on aircraft braking distance computation. In *Pavement and Asset Management*; CRC Press: Boca Raton, FL, USA, 2019; pp. 731–740. [\[CrossRef\]](#)
12. Ketabdari, M.; Toraldo, E.; Crispino, M. Assessing the impact of the slopes on runway drainage capacity based on wheel/path surface adhesion conditions. *Aviation* **2021**, *25*, 140–148. [\[CrossRef\]](#)
13. Pasindu, H.R.; Fwa, T.F.; Ong, G.P. Analytical evaluation of aircraft operational risks from runway rutting. *Int. J. Pavement Eng.* **2016**, *17*, 810–817. [\[CrossRef\]](#)

14. Alber, S.; Schuck, B.; Ressel, W.; Behnke, R.; Falla, G.C.; Kaliske, M.; Leischner, S.; Wellner, F. Modeling of surface drainage during the service life of asphalt pavements showing long-term rutting: A modular hydromechanical approach. *Adv. Mater. Sci. Eng.* **2020**, *2020*, 8793652. [[CrossRef](#)]
15. Zhang, Y.; Yuan, B.; Chou, Y. Analyzing Driving Safety Using Vehicle-Water-Filled Rutting Dynamics Model and Simulation. *Adv. Mater. Sci. Eng.* **2022**, *2022*, 9372336. [[CrossRef](#)]
16. Ketabdari, M.; Millán, I.P.; Crispino, M.; Toraldo, E.; Perneti, M. Numerical Prediction Model of Runway-Taxiway Junctions for Optimizing the Runway Evacuation Time. In *International Conference on Computational Science and Its Applications*; Springer: Cham, Switzerland, 2021; pp. 298–308. [[CrossRef](#)]
17. American Association of State Highway and Transportation Officials (AASHTO). *Highway Drainage Guidelines*; AASHTO: Washington, DC, USA, 1992.
18. Nygårdhs, S. *Aquaplaning: Development of a Risk Pond Model from Road Surface Measurements*; Linköping University: Linköping, Sweden, 2003.
19. Fwa, T.F.; Pasindu, H.R.; Ong, G.P. Critical rut depth for pavement maintenance based on vehicle skidding and hydroplaning consideration. *J. Transp. Eng.* **2012**, *138*, 423. [[CrossRef](#)]
20. Chu, L.; Fwa, T.F.; Ong, G.P. Evaluating hydroplaning potential of rutted highway pavements. *J. East. Asia Soc. Transp. Stud.* **2015**, *11*, 1613–1622. [[CrossRef](#)]
21. *ASTM D5340-11*; Standard Test Method for Airport Pavement Condition Index Surveys. American Society for Testing and Materials: West Conshohocken, PA, USA, 2012; p. 55. [[CrossRef](#)]
22. Fwa, T.F. Determination and prediction of pavement skid resistance—connecting research and practice. *J. Road Eng.* **2021**, *1*, 43–62. [[CrossRef](#)]
23. General Aviation Safety Sense Leaflet—Aeroplane Performance. In *Safety Sense Leaflet 07 Aeroplane Performance*; Civil Aviation Authority: Crawley, UK, 2013.

Disclaimer/Publisher’s Note: The statements, opinions and data contained in all publications are solely those of the individual author(s) and contributor(s) and not of MDPI and/or the editor(s). MDPI and/or the editor(s) disclaim responsibility for any injury to people or property resulting from any ideas, methods, instructions or products referred to in the content.